

# Metal–Ligand Bonding in Coinage Metal–Phosphine Complexes: The Synthesis and Structure of Some Low-Coordinate Silver(I)–Phosphine Complexes

Robert E. Bachman\* and David F. Andretta

Department of Chemistry, Box 571227, Georgetown University, Washington, D.C. 20057-1227

Received June 24, 1998

Reaction of  $\text{AgBF}_4$  with 2 equiv of  $\text{Ph}_3\text{P}$  in acetonitrile followed by recrystallization from dichloromethane/hexane yields the mixed phosphine–nitrile complex  $[(\text{Ph}_3\text{P})_2\text{AgNCCH}_3]\text{BF}_4$  (**I**) as its dichloromethane solvate,  $\text{I}\cdot 0.5\text{CH}_2\text{Cl}_2$ . This solvate crystallizes in the monoclinic space group  $C2/c$  with  $a = 22.928(5)$ ,  $b = 12.700(3)$ ,  $c = 25.156(5)$  Å,  $\beta = 97.53(3)^\circ$ , and  $Z = 8$ . The acetonitrile ligand in **I** is loosely bound to the metal center and easily lost, even in the solid state, without decomposition. Hence, recrystallization of dried samples of  $\text{I}\cdot 0.5\text{CH}_2\text{Cl}_2$  from  $\text{CH}_2\text{Cl}_2$ /hexane results in isolation of the novel low-coordinate phosphine complex  $[(\text{Ph}_3\text{P})_2\text{Ag}]\text{BF}_4$  (**II**). **II** crystallizes in the monoclinic space group  $C2/c$  with  $a = 21.733(9)$ ,  $b = 12.272(4)$ ,  $c = 24.356(9)$  Å,  $\beta = 95.01(3)^\circ$ , and  $Z = 8$ . In both cases, a weak interaction is present between a fluorine atom of the  $\text{BF}_4^-$  anion and the silver cation. However, these interactions appear to be essentially electrostatic rather than dative in nature, implying that **I** is best considered a three-coordinate silver complex and that **II** is a rare, structurally characterized example of a two-coordinate silver–phosphine complex. These solid-state geometric assignments are supported by  $^{31}\text{P}$  NMR studies, which reveal a Ag–P coupling constant of 550 Hz for **II**, consistent with the presence of a linear two-coordinate complex in solution. The NMR data also indicate that the phosphine ligands are involved in exchange processes, which are accelerated by the presence of a donor solvent such as acetonitrile. Comparison of **II** with its gold analogue supports the previously stated concept that gold atoms are smaller than silver atoms. An analysis of 13 other isostructural pairs of silver and gold complexes culled from the crystallographic database lends further support to this concept.

## Introduction

The coordination chemistry of the coinage metals has been the subject of investigation for decades.<sup>1</sup> Historically, interest in this area grew out of the diverse structural motifs displayed by these superficially similar monovalent cations. More recently, interest has been renewed by both practical and theoretical concerns. An example of the practical motivations driving research in this area is the use of such coinage metal complexes as potential precursors to metal films via CVD (chemical vapor deposition) processes.<sup>2</sup> Theoretical interest has been sparked by work which shows that these metals all display the ability to form attractive nonbonding “metallophilic” interactions that can strongly influence the structure and properties in these materials.<sup>3</sup> Calculations have shown that such interactions are most likely the result of relativistic and correlation effects,

particularly in the case of gold, for which these effects are especially pronounced.<sup>3c,4</sup> Interestingly, Schmidbaur and co-workers have recently<sup>5</sup> shown that, in at least a few cases, these relativistic effects result in gold–ligand bonds that are shorter than the corresponding silver–ligand bonds or in effect that gold atoms are smaller than silver atoms. Their calculations indicate that this counterintuitive observation should be a general structural feature for structurally related gold and silver complexes. However, while the theoretical basis for this conclusion is fairly well established, experimental verification is hindered by a lack of characterized isostructural pairs of silver(I) and gold(I) complexes. This paucity of data is the result of the tendency of these two metals to prefer different coordination geometries, linear two-coordinate for gold and tetrahedral four-coordinate for silver.<sup>1</sup> In a few cases, isostructural two-coordinate complexes have been prepared for comparison purposes by using sterically bulky ligands to enforce the geometry at silver. Unfortunately, the use of such sterically demanding ligands can produce results that are artifacts of their steric bulk rather than inherent structural features,<sup>6</sup> making any inference about the generality of the results difficult.

We now wish to report the isolation and crystallographic characterization of two new low-coordinate complexes of silver(I) with triphenylphosphine, including the first example of a

\* To whom correspondence should be addressed.

- (1) (a) Hathaway, B. J. *Comprehensive Coordination Chemistry*; Wilkinson, G., Ed.; Pergamon: Oxford, 1987; Vol. 5, pp 533–591. (b) Lancashire, R. J. *Comprehensive Coordination Chemistry*; Wilkinson, G., Ed.; Pergamon: Oxford, 1987; Vol. 5, pp 775–838. (c) Puddephatt, R. J. *Comprehensive Coordination Chemistry*; Wilkinson, G., Ed.; Pergamon: Oxford, 1987; Vol. 5, pp 862–886.
- (2) (a) Toscano, P. J.; Dettelbacher, C.; Waechter, J.; Pavri, N. P.; Hunt, D. H. *J. Coord. Chem.* **1996**, *38*, 319–335. (b) Xu, C. Y.; Hamden-Smith, M. J.; Kostas, T. T. *Chem. Mater.* **1995**, *7*, 1539–1546. (c) Yuan, Z.; Dryden, N. H.; Vittall, J. J.; Puddephatt, R. J. *Chem. Mater.* **1995**, *7*, 1696–1702. (d) Puddephatt, R. J.; Treurnicht, I. J. *Organomet. Chem.* **1987**, *319*, 129–137. (e) Holl, M. M. B.; Seidler, P. F.; Kowakzyk, S. P.; McFeely, F. R. *Inorg. Chem.* **1994**, *33*, 510–517. (f) Puddephatt, R. J. *Polyhedron* **1994**, *13*, 1233–1243.
- (3) (a) Siemeling, U.; Vorfeld, U.; Neumann, B.; Stammeler, H.-G. *Chem. Commun.* **1997**, 1723–1724. (b) Omary, M. A.; Webb, T. R.; Assefa, Z.; Shankle, G. E.; Patterson, H. H. *Inorg. Chem.* **1998**, *37*, 1380–1386. (c) Schmidbaur, H. *Chem. Soc. Rev.* **1995**, *24*, 391–400.

(4) Pykkö, P. *Chem. Rev.* **1988**, *88*, 563–594.

(5) (a) Bayler, A.; Schier, A.; Bowmaker, G. A.; Schmidbaur, H. *J. Am. Chem. Soc.* **1996**, *118*, 7006–7007. (b) Bowmaker, G. A.; Schmidbaur, H.; Krüger, S.; Röscher, N. *Inorg. Chem.* **1997**, *36*, 1754–1757. (c) Tripathi, U. M.; Bauer, A.; Schmidbaur, H. *J. Chem. Soc., Dalton Trans.* **1997**, 2865–2868.

(6) Bachman, R. E.; Schmidbaur, H. *Inorg. Chem.* **1996**, *35*, 1399–1401 and references therein.

**Table 1.** Crystallographic Data for **I**·0.5CH<sub>2</sub>Cl<sub>2</sub> and **II**

compound	<b>I</b> ·0.5CH <sub>2</sub> Cl <sub>2</sub>	<b>II</b>
empirical formula	C <sub>38.50</sub> H <sub>34</sub> AgBClF <sub>4</sub> NP <sub>2</sub>	C <sub>36</sub> H <sub>30</sub> AgBF <sub>4</sub> P <sub>2</sub>
fw	802.74	719.22
temp	−100 °C	−100 °C
cryst syst	monoclinic	monoclinic
space group	C2/c	C2/c
unit cell dimensions	<i>a</i> = 22.928(5) Å <i>b</i> = 12.700(3) Å <i>c</i> = 25.156(5) Å $\beta$ = 97.53(3)°	<i>a</i> = 21.733(9) Å <i>b</i> = 12.272(4) Å <i>c</i> = 24.356(9) Å $\beta$ = 95.01(3)°
volume	7262.3(25) Å <sup>3</sup>	6471.1(42) Å <sup>3</sup>
Z	8	8
density (calculated)	1.468 g/cm <sup>3</sup>	1.476 g/cm <sup>3</sup>
absorption coeff	0.766 mm <sup>−1</sup>	0.770 mm <sup>−1</sup>
<i>F</i> (000)	3256	2912
cryst size	0.32 × 0.30 × 0.22 mm <sup>3</sup>	0.48 × 0.25 × 0.08 mm <sup>3</sup>
$\theta$ range for data collection	1.63–28.33°	1.68–28.31°
reflns collected	30 109	26 688
indep reflns	8834 [ <i>R</i> (int) = 0.0346]	7863 [ <i>R</i> (int) = 0.0744]
data/param	8834/611	7859/572
final <i>R</i> indices	<i>R</i> 1 = 0.0324, <i>wR</i> 2 = 0.0716	<i>R</i> 1 = 0.0604, <i>wR</i> 2 = 0.1316
goodness of fit (GOF)	1.065	1.147
extinction coeff	0.00017(3)	0.00012(5)
largest diff peak and hole	0.604 and −0.485 e Å <sup>−3</sup>	1.067 and −1.304 e Å <sup>−3</sup>

structurally characterized two-coordinate phosphine complex of silver, [(Ph<sub>3</sub>P)<sub>2</sub>Ag]<sup>+</sup>, without the use of sterically bulky ligands. The isolation of this species, for which there is a well-characterized gold analogue, allows for the direct comparison of Ag–P and Au–P bonding parameters, without the complications related to the use of sterically bulky ligands. Our experimental results also prompted us to conduct a search of the crystallographic database for other isostructural silver and gold complexes. This search yielded 13 additional isostructural pairs of complexes with varying coordination geometries ranging from linear to tetrahedral. Comparison of these pairs strongly indicates that the conclusions reached by Schmidbaur et al.<sup>5</sup> on the basis of their more limited data are completely general.

### Experimental Procedures

**Preparation of [(Ph<sub>3</sub>P)<sub>2</sub>AgNCCH<sub>3</sub>]BF<sub>4</sub> (I).** Under a nitrogen atmosphere, 0.68 g of AgBF<sub>4</sub> (3.5 mmol) was dissolved in 15 mL of dry CH<sub>3</sub>CN. A solution of 1.83 g (7.0 mmol) of Ph<sub>3</sub>P in 40 mL of CH<sub>3</sub>CN was then added in one portion. The mixture was swirled briefly by hand to ensure complete mixing and then allowed to stand for 90 min before the solvent was removed in vacuo to produce an opaque oil, which slowly solidified on standing. This oil, or glassy solid, was redissolved in CH<sub>2</sub>Cl<sub>2</sub> (25 mL), and hexane was added dropwise to the cloud point. Initially an oil began to separate from the solution; however, crystallization was induced by cooling the mixture to 0 °C overnight. X-ray quality crystals of **I**·0.5CH<sub>2</sub>Cl<sub>2</sub> were isolated by decanting the supernatant to yield 2.60 g (92.5% based on Ag) of product: mp (uncorrected) 193.5–195 °C; <sup>1</sup>H NMR (CDCl<sub>3</sub>, ppm) 7.55–7.30 (m, 30H), 5.32 (s, 1H), 2.01 (s, 3H); <sup>31</sup>P NMR (CDCl<sub>3</sub>, ppm) 14 (d, <sup>1</sup>*J*<sub>Ag–P</sub> = 404 Hz); IR (KBr, cm<sup>−1</sup>) 2292, 2258.

**Structural Study of I·0.5CH<sub>2</sub>Cl<sub>2</sub>.** A block approximately 0.32 × 0.30 × 0.22 mm<sup>3</sup> in size was cut from a larger crystal and mounted on a glass fiber using epoxy cement. All X-ray data were collected on a Siemens SMART CCD system at −100 °C. The initial unit cell was determined using a least-squares analysis of a random set of reflections collected from three series of 0.3° wide  $\omega$  scans (20 frames/series), which were well distributed in reciprocal space. The intensity data were then collected with 0.3° wide  $\omega$  scans and a crystal-to-detector distance of 5.0 cm, providing a complete sphere of data to a maximum resolution of 0.75 Å ( $2\theta_{\max}$  = 56.66°). The data were corrected for Lorentz and polarization effects as well as absorption. The empirical absorption correction was made on the basis of equivalent reflection measurements using Blessing's method as incorporated into the program

**Table 2.** Atomic Coordinates (×10<sup>4</sup>) and Equivalent Isotropic Displacement Parameters (Å<sup>2</sup> × 10<sup>3</sup>) for Selected Atoms of **I**·0.5CH<sub>2</sub>Cl<sub>2</sub>

	<i>x</i>	<i>y</i>	<i>z</i>	<i>U</i> (eq)
Ag(1)	1918(1)	6322(1)	1202(1)	27(1)
P(2)	2197(1)	4707(1)	775(1)	24(1)
P(1)	1051(1)	7426(1)	979(1)	27(1)
N(1)	2680(1)	7041(2)	1790(1)	52(1)
C(1)	2862(1)	7270(2)	2211(1)	47(1)
C(2)	3087(3)	7559(3)	2762(2)	76(1)
B(1)	1636(2)	5414(3)	2493(1)	53(1)
F(1)	1554(4)	5091(7)	1975(3)	75(2)
F(2)	1266(4)	4683(6)	2759(3)	67(2)
F(3)	2204(3)	5087(6)	2683(3)	77(2)
F(4)	1462(4)	6360(6)	2571(3)	127(3)
F(1A)	1727(5)	5079(6)	2000(4)	97(4)
F(2A)	1232(6)	5099(8)	2704(5)	108(4)
F(3A)	2148(5)	5578(9)	2840(3)	101(3)
F(4A)	1530(3)	6533(7)	2326(3)	78(2)

SADABS.<sup>7</sup> The structure was solved using direct methods and refined on *F*<sup>2</sup> by full-matrix least-squares methods using the SHELXTL/PC (v. 5.03) package.<sup>8</sup> All non-hydrogen atoms were refined anisotropically, while the hydrogen atoms were refined isotropically. During the later stages of refinement, the fluorine atoms of the [BF<sub>4</sub>]<sup>−</sup> anion were found to be disordered and were modeled using two positions for each atom with a relative (refined) occupancy of 0.55/0.45. The final refinement converged with residuals of *wR*2(*F*<sup>2</sup>) = 0.0716 (all data), *R*1(*F*) = 0.0324 (*I* > 2 $\sigma$ (*I*)), and GOF = 1.065. All relevant crystallographic information is included in Table 1, selected atomic coordinates and equivalent isotropic displacement parameters are reported in Table 2, and the significant bond metrics are compiled in Table 3.

**Thermal Analysis of I·0.5CH<sub>2</sub>Cl<sub>2</sub>.** Differential scanning calorimetry (DSC) was performed on a small (~12 mg) sample of **I**·0.5CH<sub>2</sub>Cl<sub>2</sub>, which was removed directly from the mother liquor and dried briefly on a piece of filter paper. The measurement was carried out under a dynamic N<sub>2</sub> purge using a heating rate of 5 °C/min to a maximum temperature of 225 °C. Three endothermic processes were observed at (maximum signal values) 92.8, 103.0, and 204.0 °C. Thermogravimetric analysis was performed on another sample (~11.5

- (7) (a) Blessing, R. H. *Acta Crystallogr.* **1995**, A51, 33–38. (b) Sheldrick, G. M. *SADABS* "Siemens Area Detector Absorption Correction"; Universität Göttingen: Göttingen, Germany, 1996.  
(8) *SHELXTL-PC*, version 5.03; Siemens Analytical Instruments: Madison, WI.

**Table 3.** Selected Bond Distances (Å) and Angles (deg) for **I**·0.5CH<sub>2</sub>Cl<sub>2</sub>

Ag(1)–N(1)	2.321(2)	P(1)–C(121)	1.828(2)
Ag(1)–P(1)	2.4389(7)	P(1)–C(131)	1.822(2)
Ag(1)–P(2)	2.4395(7)	P(2)–C(211)	1.828(2)
N(1)–C(1)	1.126(3)	P(2)–C(221)	1.818(2)
C(1)–C(2)	1.461(4)	P(2)–C(231)	1.824(2)
P(1)–C(111)	1.819(2)		
N(1)–Ag(1)–P(1)	116.37(6)	C(121)–P(1)–Ag(1)	114.52(8)
N(1)–Ag(1)–P(2)	113.11(6)	C(131)–P(1)–Ag(1)	108.31(7)
P(1)–Ag(1)–P(2)	129.37(2)	C(221)–P(2)–C(231)	104.31(10)
Ag(1)–N(1)–C(1)	148.9(2)	C(221)–P(2)–C(211)	103.04(10)
N(1)–C(1)–C(2)	178.7(4)	C(231)–P(2)–C(211)	105.25(10)
C(111)–P(1)–C(131)	104.42(10)	C(221)–P(2)–Ag(1)	119.15(7)
C(111)–P(1)–C(121)	104.92(10)	C(231)–P(2)–Ag(1)	110.21(7)
C(131)–P(1)–C(121)	105.28(11)	C(211)–P(2)–Ag(1)	113.60(7)
C(111)–P(1)–Ag(1)	118.22(8)		

**Table 4.** Atomic Coordinates ( $\times 10^4$ ) and Equivalent Isotropic Displacement Parameters ( $\text{Å}^2 \times 10^3$ ) for Selected Atoms of **II**

	x	y	z	U (eq)
Ag(1)	2644(1)	4837(1)	1249(1)	27(1)
P(1)	1669(1)	3894(1)	1066(1)	24(1)
P(2)	3478(1)	6052(1)	1065(1)	24(1)
B(1)	3442(2)	2789(5)	2395(2)	36(1)
F(1)	3105(1)	3551(2)	2068(1)	51(1)
F(2)	3340(12)	3070(23)	2936(9)	60(6)
F(2A)	3177(6)	2460(19)	2831(6)	55(4)
F(2B)	3560(29)	3287(38)	2874(16)	99(25)
F(3)	3251(12)	1749(16)	2320(13)	86(10)
F(3A)	3499(10)	1955(13)	2019(6)	72(4)
F(3B)	3077(16)	1861(35)	2500(27)	61(14)
F(4)	4068(13)	2829(29)	2368(15)	89(15)
F(4A)	4016(6)	3218(14)	2524(8)	47(6)
F(4B)	3978(29)	2407(67)	2166(19)	95(23)

mg) handled in a manner identical to that used for the DSC study. Two overlapping weight loss processes were observed between 85 and 120 °C. The total weight loss for both processes was 10.3% (theoretical weight change for complete loss of both CH<sub>2</sub>Cl<sub>2</sub> and CH<sub>3</sub>CN equals 10.4%). No other processes involving a change in weight were observed up to 210 °C.

**Isolation and Structure of [(Ph<sub>3</sub>P)<sub>2</sub>Ag]BF<sub>4</sub> (II).** A small sample (~250 mg) of **I**·0.5CH<sub>2</sub>Cl<sub>2</sub>, which had been stored for several weeks as a solid, was redissolved in 1–2 mL of CH<sub>2</sub>Cl<sub>2</sub>. Hexane was then added dropwise to the cloud point, and the mixture was allowed to stand at room temperature for a few minutes, resulting in the formation of X-ray quality crystals. The absence of both the dichloromethane solvent and the acetonitrile ligand in this bulk sample was confirmed by <sup>1</sup>H NMR and IR spectroscopy. Collection and reduction of the crystallographic data were performed in a manner identical to that described above. Likewise, the structure solution and refinement were carried out in a similar manner. During the latter stages of refinement, the [BF<sub>4</sub>]<sup>−</sup> anion was found to display rotational disorder around the B(1)–F(1) vector. The disorder was modeled using three positions for each atom of equal (0.33) occupancy. The refinement converged with residuals of wR<sub>2</sub> = 0.1316, R<sub>1</sub> = 0.0604, and GOF = 1.147. The crystallographic details are compiled in Table 1, and selected atomic coordinates and equivalent isotropic displacement parameters are presented in Table 4. The significant bond metrics are reported in Table 5.

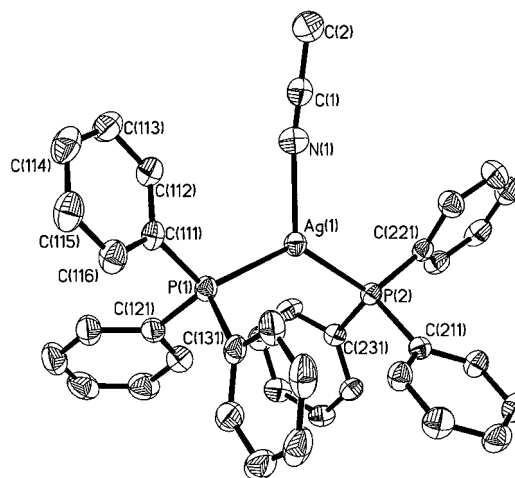
Other spectroscopic and analytical data for **II** include the following: mp (uncorrected) 198.0–199.5 °C; <sup>1</sup>H NMR (CDCl<sub>3</sub>, ppm) 7.55–7.30 m; <sup>31</sup>P NMR (CDCl<sub>3</sub>, ppm) 14 (d, <sup>1</sup>J<sub>Ag–P</sub> = 550 Hz); IR (KBr, cm<sup>−1</sup>) no absorptions were observed between 2600 and 1600 cm<sup>−1</sup>.

## Results

The reaction of 2 equiv of triphenylphosphine with silver tetrafluoroborate in acetonitrile followed by recrystallization of this oil from dichloromethane and hexane produces colorless crystals of [(Ph<sub>3</sub>P)<sub>2</sub>AgNCCH<sub>3</sub>][BF<sub>4</sub>] (**I**) (Figure 1) in excellent

**Table 5.** Selected Bond Distances (Å) and Angles (deg) for **II**

Ag(1)–P(2)	2.4177(12)	P(1)–C(131)	1.824(4)
Ag(1)–P(1)	2.4219(13)	P(2)–C(221)	1.810(4)
P(1)–C(121)	1.810(4)	P(2)–C(231)	1.814(4)
P(1)–C(111)	1.822(4)	P(2)–C(211)	1.822(4)
P(2)–Ag(1)–P(1)	156.65(4)	C(221)–P(2)–C(231)	105.2(2)
C(121)–P(1)–C(111)	105.0(2)	C(221)–P(2)–C(211)	106.0(2)
C(121)–P(1)–C(131)	104.6(2)	C(231)–P(2)–C(211)	104.0(2)
C(111)–P(1)–C(131)	104.4(2)	C(221)–P(2)–Ag(1)	118.05(14)
C(121)–P(1)–Ag(1)	119.02(14)	C(231)–P(2)–Ag(1)	113.11(13)
C(111)–P(1)–Ag(1)	110.18(14)	C(211)–P(2)–Ag(1)	109.32(14)
C(131)–P(1)–Ag(1)	112.45(14)		

**Figure 1.** Diagram showing the cation of **I**·0.5CH<sub>2</sub>Cl<sub>2</sub> with the displacement ellipsoids at 50% probability. The solvent molecule, anion, and hydrogen atoms have been omitted for clarity. The numbering scheme for all the phenyl rings follows the scheme shown for the numbered ring.

yield as a dichloromethane solvate, **I**·0.5CH<sub>2</sub>Cl<sub>2</sub>. The crystals produced in this fashion are of X-ray quality, allowing for direct confirmation of the structure by crystallography. The unit cell is composed of eight cation–anion pairs and four molecules of dichloromethane (residing on 2-fold axes). While the solvent molecules make no short contacts with either the cation or anion, the cations and anions appear to be loosely associated via weak electrostatic interactions. The essential crystallographic details can be found in Table 1, and the important bond metrics are compiled in Table 3.

<sup>1</sup>H NMR spectroscopy of fresh samples of **I**·0.5CH<sub>2</sub>Cl<sub>2</sub> shows the presence of both the acetonitrile and dichloromethane, as well as the aromatic signals from the phosphine ligands. The integrated intensities for these signals are in good agreement with expectations based on the observed solid-state structure. The <sup>31</sup>P NMR spectrum of **I** consists of a doublet of broad peaks centered at 14 ppm. As a result of the broad nature of these peaks, it is not possible to resolve the individual <sup>107</sup>Ag and <sup>109</sup>Ag coupling constants, but an average coupling constant (<sup>1</sup>J<sub>Ag–P</sub>) can be estimated as 404 Hz. In addition to the <sup>1</sup>H NMR data, solid-state IR spectroscopy also confirms the presence of the acetonitrile ligand with absorptions at 2292 and 2258 cm<sup>−1</sup>, compared with 2292 and 2252 cm<sup>−1</sup> for pure acetonitrile.

The acetonitrile ligand of **I**, along with the dichloromethane of solvation, is readily lost from the solid material with no noticeable decomposition to produce [(Ph<sub>3</sub>P)<sub>2</sub>Ag]BF<sub>4</sub> (**II**). This ligand elimination process occurs spontaneously from crystalline samples of **I**·0.5CH<sub>2</sub>Cl<sub>2</sub> stored under ambient conditions for several days. Alternatively, thermal analysis studies indicate that the same result may be achieved by heating the material to

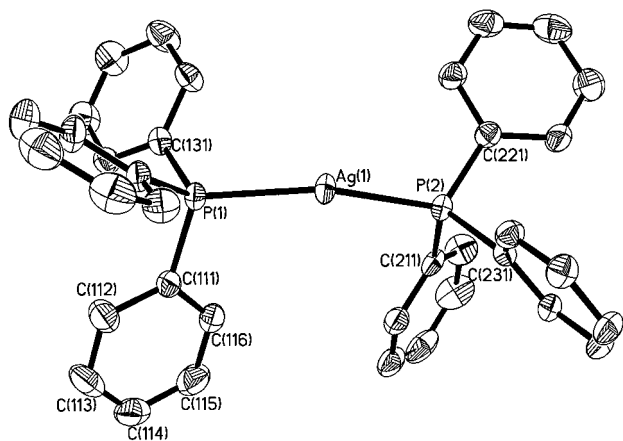


**Figure 2.** Diagram showing the cation of **II** with the displacement ellipsoids at 50% probability. The anion and hydrogen atoms have been omitted for clarity. The numbering scheme for all the phenyl rings follows the scheme shown for the numbered ring.

approximately 110 °C for a short period of time (15–20 min). The  $^1\text{H}$  NMR spectrum of samples of **II** produced by either method shows an almost complete loss of the signals attributable to the acetonitrile and the dichloromethane. The IR absorptions due to the acetonitrile ligand are also absent from these samples. The  $^{31}\text{P}$  spectrum of these samples remains a broad doublet centered at 14 ppm; however, the peak widths narrow slightly, and the averaged Ag–P coupling constant increases to 530 Hz.

Recrystallization of crude **II** from  $\text{CH}_2\text{Cl}_2/\text{hexane}$  yields colorless X-ray quality crystals. After recrystallization, no signals attributable to either acetonitrile or dichloromethane are detectable by  $^1\text{H}$  NMR. The doublet observed in the  $^{31}\text{P}$  spectrum remains centered at 14 ppm, with a further decrease in peak widths and a concurrent increase in the Ag–P coupling constant to 550 Hz. The structure of **II** was confirmed crystallographically (Figure 2). As with **I**, the unit cell of **II** consists of eight weakly associated cation–anion pairs. The key crystallographic parameters for **II** are compiled in Table 1, and the important bond metrics are listed in Table 5.

## Discussion

Upon removal of the acetonitrile, a 2:1 mixture of triphenylphosphine and silver tetrafluoroborate initially yields an oily semisolid material, which we were not able to identify unambiguously but which most likely has the general formulation  $[(\text{Ph}_3\text{P})_2\text{Ag}(\text{NCCH}_3)_n\text{BF}_4]$ ,  $n = 0-2$ . Recrystallization of this material from  $\text{CH}_2\text{Cl}_2/\text{hexane}$  produces crystalline samples of **I**·0.5 $\text{CH}_2\text{Cl}_2$  in essentially quantitative yield. Allowing a solid sample of **I**·0.5 $\text{CH}_2\text{Cl}_2$  to stand for several days or heating it to approximately 110 °C for a short time leads to a loss of both the NMR and IR signals associated with the acetonitrile and dichloromethane. This conversion of **I** to **II** takes place with no noticeable decomposition; moreover, **II** is stable indefinitely, even if no precautions are taken to protect it against light or atmospheric moisture. The high degree of stability found for **II** is somewhat surprising in light of the reported light sensitivity of other low-coordinate silver complexes such as  $[(\text{Mes}_3\text{P})_2\text{Ag}]\text{PF}_6$  (**III**)<sup>9</sup> and  $(\text{Ph}_3\text{P})_n\text{AgNO}_3$  ( $n = 1-4$ ).<sup>10</sup> Indeed, samples

**Table 6.** Comparison of Ag–P Bond Lengths for Representative Aromatic Phosphine–Silver(I) Complexes<sup>a</sup>

compd	av Ag–P distance (Å)	ref
$(\text{Ph}_3\text{P})\text{AgNO}_3$	2.369	11
$[\text{Ph}_3\text{P}\text{AgCl}]_4$	2.382	12
<b>II</b>	2.4198	this work
$(\text{Ph}_3\text{P})_2\text{AgNO}_3$	2.434	10
<b>I</b>	2.4392	this work
$[(\text{Mes}_3\text{P})_2\text{Ag}]^+$	2.451	5a, 9
$[\text{Ph}_3\text{P}\text{Ag}]_4$	2.452	13
$(\text{Ph}_3\text{P})_2\text{AgBr}$	2.458	14
$[(\text{Ph}_3\text{P})_2\text{AgCl}]_2$	2.476	14, 15
$[(\text{Ph}_3\text{P})_2\text{AgBr}]_2$	2.496	14
$(\text{Ph}_3\text{P})_3\text{AgBr}$	2.535	16
$[(\text{Ph}_3\text{P})_3\text{Ag}]\text{BF}_4$	2.542	17
$(\text{Ph}_3\text{P})_3\text{AgCl}$	2.557	16, 18
$(\text{Ph}_3\text{P})_3\text{Ag}(\text{NCS})$	2.565	19
$[(\text{Ph}_3\text{P})_3\text{Ag}]\text{NO}_3$	2.567	10a
$(\text{Ph}_3\text{P})_3\text{AgI}$	2.604	16, 17, 20
$[(\text{Ph}_3\text{P})_4\text{Ag}]^+$	2.658	10a, 21

<sup>a</sup> Values are listed in order of increasing length.

of **II** can be recrystallized repeatedly from  $\text{CH}_2\text{Cl}_2/\text{hexane}$  with no apparent degradation.

As the highly crystalline nature of these two structurally related compounds offers a unique opportunity to examine how coordination number and geometry affect the metal–ligand bonding, we undertook crystallographic studies of both species. The Ag–P bond distances in **I**, 2.4395(7) and 2.4389(7) Å, lie at the short end of the range observed to date for silver–phosphine complexes (Table 6) and, interestingly, are measurably shorter than those observed for the two-coordinate complex **III** (av 2.451 Å).<sup>5a,9</sup> The loss of the nitrile ligand causes a small contraction of the Ag–P distances in **II** to 2.4177(12) and 2.4219(13) Å. This latter pair of values is among the shortest that have been observed for silver–phosphine complexes, with the most comparable distances being monophosphine complexes such as  $[\text{Ph}_3\text{P}\text{AgCl}]_4$  (2.382 Å) and  $\text{Ph}_3\text{P}\text{AgNO}_3$  (2.369 Å). Since **II** and **III** are essentially structural analogues (vide infra), differing primarily in the identity of the aryl groups on the phosphine ligands, the difference in bond lengths between these two complexes (0.031 Å) can be taken as a measure of the bond lengthening caused by the steric repulsion of the methyl groups in the  $\text{Mes}_3\text{P}$  ligand.

In contrast to the short Ag–P bonds in **I**, the Ag–N distance (2.321(2) Å) is significantly longer than that observed for  $[\text{Ag}(\text{NCCH}_3)_4][\text{BF}_4]$  (2.266 Å),<sup>22</sup> the only other structurally characterized nitrile complex of silver. The weak nature of this interaction is supported by the solid-state IR data, which show

(9) (a) Alyea, E. C.; Ferguson, G.; Somogyvari, A. *Inorg. Chem.* **1982**, *21*, 1369–1371. (b) Alyea, E. C.; Dias, S. A.; Stevens, S. *Inorg. Chim. Acta* **1980**, *44*, L203–L204.  
 (10) (a) Barron, P. F.; Dyason, J. C.; Healy, P. C.; Engelhardt, L. M.; Skelton, B. W.; White, A. H. *J. Chem. Soc., Dalton Trans.* **1986**, 1965–1970. (b) Harker, C. S. W.; Tiekink, E. R. T. *Acta Crystallogr.* **1989**, *C45*, 1815–1817.

(11) Stein, R. A.; Knobler, C. *Inorg. Chem.* **1977**, *16*, 242–245.  
 (12) Teo, B.-K.; Calabrese, J. C. *Inorg. Chem.* **1976**, *15*, 2467–2474.  
 (13) Teo, B.-K.; Calabrese, J. C. *Inorg. Chem.* **1976**, *15*, 2474–2486.  
 (14) Bowmaker, G. A.; Effendy, Hanna, J. V.; Healy, P. C.; Skelton, B. W.; White, A. H. *J. Chem. Soc., Dalton Trans.* **1993**, 1387–1397.  
 (15) Cassell, A. *Acta Crystallogr.* **1979**, *B35*, 174–177.  
 (16) Engelhardt, L. M.; Healy, P. C.; Patrick, V. A.; White, A. H. *Aust. J. Chem.* **1987**, *40*, 1873–80.  
 (17) Camalli, M.; Caruso, F. *Inorg. Chim. Acta* **1987**, *127*, 209–213.  
 (18) Cassel, A. *Acta Crystallogr.* **1981**, *B37*, 229–231.  
 (19) Othman, A. H.; Fun, H.-K.; Sivakumar, K.; Farina, Y.; Baba, I. *Acta Crystallogr.* **1996**, *C52*, 1933–1935.  
 (20) Hibbs, D. E.; Hursthouse, M. B.; Malik, K. M. A.; Beckett, M. A.; Jones, P. W. *Acta Crystallogr.* **1996**, *C52*, 884–887.  
 (21) (a) Engelhardt, L. M.; Pakawatchai, C.; White, A. H.; Healy, P. C. *J. Chem. Soc., Dalton Trans.* **1985**, 125–133. (b) Cotton, F. A.; Luck, R. L. *Acta Crystallogr.* **1989**, *C45*, 1222–1224. (c) Bowmaker, G. A.; Healy, P. C.; Engelhardt, L. M.; Kildea, J. D.; Skelton, B. W.; White, A. H. *Aust. J. Chem.* **1990**, *43*, 1697–1705.  
 (22) Jones, P. G.; Bembek, E. Z. *Kristallogr.* **1993**, *208*, 213–218.

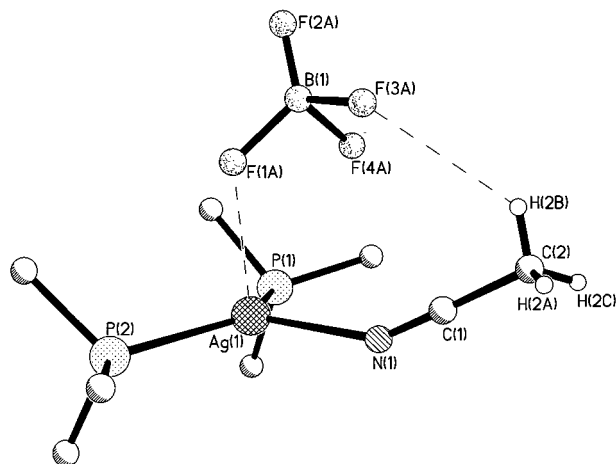


**Figure 3.** Diagram showing the relative orientation of the silver atom, the acetonitrile ligand, and the  $[\text{BF}_4]^-$  ion in the solid state for  $\text{I} \cdot 0.5\text{CH}_2\text{Cl}_2$ . Only the ipso carbons of the phenyl rings are included for clarity. The dashed lines indicate the closest contacts between the fluorine atoms and the silver and hydrogen atoms of the acetonitrile ligand.

very little shift in the C–N stretching frequencies in comparison with those for pure acetonitrile, and the ease by which the ligand is lost from the metal center's coordination sphere. Another interesting feature of the Ag–N bonding is the significant deviation of the Ag–N–C bond angle ( $148.9(2)^\circ$ ) from linearity. This nonlinearity is contrary to expectations based on simple hybridization arguments and the bond angles observed for  $[(\text{CH}_3\text{CN})_4\text{Ag}]^+$ , which range from  $166.3^\circ$  to  $179.7^\circ$ . The key to understanding this unusual feature is to consider the relative locations of the cation and the anion in the solid state. The bend in the Ag–N–C angle is such that the acetonitrile moiety is canted in the direction of the  $[\text{BF}_4]^-$  anion (Figure 3). The resulting orientation produces a short intermolecular contact ( $2.65 \text{ \AA}$ ) between one of the slightly acidic methyl protons of the acetonitrile ligand and a fluorine atom of the  $[\text{BF}_4]^-$  anion. This distance is within the range expected for hydrogen bonding;<sup>23</sup> hence, it seems logical to attribute this structural feature to hydrogen bonding rather than any unusual electronic interaction between the ligand and the metal center.

As is often the case for weakly coordinating anions such as tetrafluoroborate, the assignment of the coordination number (and geometry) of the metal centers in **I** and **II** is somewhat ambiguous. This problem arises because the anion's position relative to the cation indicates some form of weak interaction between the two ions; however, it is possible to interpret this interaction as either a very weak dative bond or simply an electrostatic attraction. In the cases of both **I** and **II**, we favor the latter interpretation for several reasons. Discounting the  $[\text{BF}_4]^-$  anion, the coordination geometry at the silver atom in **I** is essentially trigonal planar. The silver atom lies only slightly ( $0.15 \text{ \AA}$ ) above the P–P–N plane, and the sum of the angles around the silver atom is  $358.8^\circ$ . In a similar vein, the P–Ag–P in **II** ( $156.65(4)^\circ$ ) is significantly larger than that observed in three-coordinate species such as  $(\text{Ph}_3\text{P})_2\text{AgBr}$  ( $124.14(5)^\circ$ ). Indeed, the angle observed in **II** is most similar to that observed in its gold analogue  $[(\text{Ph}_3\text{P})_2\text{Au}]\text{BF}_4$  ( $167.3(1)^\circ$ ).<sup>24</sup> It is also worth noting that the P–Ag–P angle in **I** ( $129.37(2)^\circ$ ) is very

similar to that observed in  $(\text{Ph}_3\text{P})_2\text{AgBr}$ . The behavior of the silver–fluorine interaction also supports the proposed bonding model. The shortest Ag–F distance in **I** ( $2.65 \text{ \AA}$ ) is significantly larger than the sum of the covalent radii ( $2.08 \text{ \AA}$ ).<sup>25</sup> Furthermore, in contrast to the decrease in Ag–P distances seen moving from **I** to **II**, the shortest Ag–F distance actually increases slightly to  $2.67 \text{ \AA}$ . If the Ag–F interaction were of a dative nature (like the Ag–P interactions), it is reasonable to expect a shortening of this distance rather than the observed effect. The electrostatic model presented here is in apparent conflict with the dative model previously invoked for  $[(\text{Ph}_3\text{P})_3\text{Ag}]\text{BF}_4$  (**IV**).<sup>17</sup> However, comparison of the two structures indicates that the interaction in **IV** is more directional and hence probably more dative in nature than that observed for **I**. While the Ag–F distance in **IV** ( $2.82 \text{ \AA}$ ) is slightly longer than that observed for **I**, **IV** displays a greater degree of pyramidity than **I**. The sum of the angles around the silver atom in **IV** is only  $353.2^\circ$ , and the Ag atom is displaced more than twice as far ( $0.39 \text{ \AA}$ ) from the P–P–P plane, with the direction of the displacement being toward a fluorine atom.

In light of the weak nature of the dative Ag–N bond in **I** and the electrostatic nature of the silver–fluorine interactions in both **I** and **II**, we decided to probe the coordination environment of the silver atom in solution for both species using  $^{31}\text{P}$  NMR. Both **I** and **II** display almost identical spectra in chloroform consisting of a single broad doublet centered near 14 ppm. Interestingly, while the chemical shift is invariant, the average Ag–P coupling constant is extremely sensitive to both the identity (**I** vs **II**) and history of the sample. Freshly crystallized samples of **I** display the smallest coupling constant, 404 Hz; however, the coupling constant increases as the material ages and loses the acetonitrile ligand from the silver's coordination sphere. Samples that are 1–2 weeks old, which show only a small percentage ( $\sim 5\%$ ) of the original acetonitrile by  $^1\text{H}$  NMR, typically display a coupling constant of approximately 530 Hz. Recrystallization of such "aged" samples to produce **II** results in a complete removal of any residual acetonitrile and an increase in the coupling constant to its maximum value of 550 Hz. This process is, in principle, reversible, and indeed, the addition of aliquots of acetonitrile to solutions of **II** causes a gradual broadening of the peak widths and a decrease in the Ag–P coupling constant. When sufficient acetonitrile has been added (2–3 equiv), the signals collapse into a very broad singlet still centered at 14 ppm. Consistent with this result, only a broad singlet is observed when a spectrum of **I** or **II** is measured in  $\text{CD}_3\text{CN}$ . The broad nature of the phosphorus signals observed for **I** and **II** is consistent with a ligand exchange process that is reasonably fast in relation to the NMR time scale. The solvent dependence of this exchange process seems to indicate that it involves the binding of an external Lewis base to the silver center to create an intermediate of increased coordination number. These observations are similar to those reported by Muetterties and Alegranti in their study of low-coordinate silver–phosphine and silver–phosphite complexes in solution.<sup>26</sup>

Silver–phosphorus coupling constants have been used by several research groups to examine the coordination geometry around the silver center both in solution and the solid state.<sup>9b,10,14,17,26,27</sup> In all these studies, the magnitude of this coupling constant is negatively correlated with the coordination number of the silver center. The value observed for **II** (530 Hz) agrees well with that seen for other two-coordinate species,

(23) (a) Pimentel, G. C.; McClellan, A. L. *The Hydrogen Bond*; W. H. Freeman: San Francisco, 1960; pp 285–293. (b) *International Tables For X-ray Crystallography*; MacGillivray, C. H.; Rieck, G. D., Eds.; D. Reidel Publishing: Dordrecht, 1985; Vol. III, p 273.

(24) Wang, J.-C. *Acta Crystallogr.* **1996**, C52, 611–613.

(25) Bondi, A. *J. Phys. Chem.* **1964**, 68, 441–451.

(26) Muetterties, E. L.; Alegranti, C. W. *J. Am. Chem. Soc.* **1972**, 94, 6386–6391.

such as **III** (552 Hz)<sup>9b</sup> and [(p-Tol<sub>3</sub>P)<sub>2</sub>Ag]<sup>+</sup> (496 Hz).<sup>26</sup> In contrast, fresh samples of **I** yield a coupling constant (404 Hz) closer to those seen for (Ph<sub>3</sub>P)<sub>2</sub>AgBr (394 Hz)<sup>14</sup> and [(Ph<sub>3</sub>P)<sub>3</sub>-Ag]BF<sub>4</sub> (318 Hz),<sup>17</sup> while aged samples of **I** (which contain small amounts of CH<sub>3</sub>CN) show an intermediate value. On the basis of these data, it is reasonable to conclude that contact between the [BF<sub>4</sub>]<sup>-</sup> anion and the silver center is lost on dissolution of the solid material, producing three- and two-coordinate cations for **I** and **II**, respectively. Such solution behavior is consistent with the electrostatic solid-state model presented above.

As noted earlier, **II** bears a strong structural similarity to its gold analogue [(Ph<sub>3</sub>P)<sub>2</sub>Au]X (X = BF<sub>4</sub><sup>-</sup>, PF<sub>6</sub><sup>-</sup>, NO<sub>3</sub><sup>-</sup>),<sup>24,27</sup> offering an additional experimental opportunity to test the idea recently proposed by Schmidbaur et al. that the covalent radius of gold is smaller than that of silver. Comparison of the average M–P bond distances (Table 7) for the [(Ph<sub>3</sub>P)<sub>2</sub>Au]<sup>+</sup> cations and for **II** reveals that the average Ag–P bond length is indeed 0.105 Å longer than the average Au–P bond length. This difference is similar to that reported for the corresponding [(Mes<sub>3</sub>P)<sub>2</sub>M]<sup>+</sup> cations<sup>5a</sup> (0.088 Å) as well as the value reported on the basis of relativistic theory (0.093 Å).<sup>5b</sup>

If the trend seen for the Ph<sub>3</sub>P and Mes<sub>3</sub>P systems is indeed due to gold having a smaller covalent radius than silver, a similar trend should be observed for all isostructural complexes of gold and silver, regardless of coordination geometry. To test this hypothesis as fully as possible, we have conducted a search of the Cambridge Structural Database for isostructural pairs of silver and gold phosphine complexes with coordination numbers ranging from 2 to 4. Before discussion of the results of this search, it is worth examining at least one of the criteria used in the selection of the isostructural pairs. Comparison of the Au–P bond lengths in the three structures determined for [(Ph<sub>3</sub>P)<sub>2</sub>-

**Table 7.** Comparison of Average Metal–Phosphorus Bond Lengths (Å) for Pairs of Structurally Related Complexes of Gold and Silver

structure type	Ag	Au	Δ <sup>a</sup>	ref (Ag/Au)
Coord. No. = 4				
[(Ph <sub>3</sub> P) <sub>4</sub> M] <sup>+</sup>	2.658	2.532	0.126	10a, 21/28
(Ph <sub>3</sub> P) <sub>3</sub> MCl	2.557	2.410	0.147	16, 18/29
(Ph <sub>3</sub> P) <sub>3</sub> M(NCS/SCN) <sup>b</sup>	2.565	2.396	0.169	19/30
[(dppe) <sub>2</sub> M] <sup>+</sup>	2.515	2.400	0.115	31/32
Coord. No. = 3				
[(Ph <sub>3</sub> P) <sub>3</sub> M] <sup>+</sup>	2.542	2.384	0.158	10a, 17/33
(Ph <sub>3</sub> P) <sub>2</sub> MBr	2.458	2.323	0.135	14/34
[N(CH <sub>2</sub> CH <sub>2</sub> PPh <sub>2</sub> )M] <sup>+</sup>	2.464	2.360	0.104	35/35
Coord. No. = 2				
[(Ph <sub>3</sub> P) <sub>2</sub> M] <sup>+</sup>	2.420	2.315	0.105	this work/25, 27
[(Mes <sub>3</sub> P) <sub>2</sub> M] <sup>+</sup>	2.451	2.352	0.099	5a, 9/5a
[(Ph <sub>2</sub> MeP) <sub>2</sub> M] <sup>+</sup>	2.4106	2.316	0.095	36/37
[(Cy <sub>3</sub> P) <sub>2</sub> M] <sup>+</sup>	2.430	2.323	0.107	38/39
[(tcep) <sub>2</sub> M] <sup>+</sup>	2.3832	2.314	0.069	40/41
[(dmpm) <sub>2</sub> M <sub>2</sub> ] <sup>2+</sup>	2.383	2.298	0.085	42/43
Ph <sub>3</sub> PMNO <sub>3</sub>	2.369	2.204	0.165	11/44

<sup>a</sup> Δ = d<sub>(Ag–P)</sub> – d<sub>(Au–P)</sub>. <sup>b</sup> These two complexes are linkage isomers with the following connectivity: AgNCS and AuSCN.

Au]<sup>+</sup>, differing only in the identity of the counterion, shows a maximum bond length variation of 0.013 Å, while the two structural studies of [(Mes<sub>3</sub>P)<sub>2</sub>Ag]<sup>+</sup>, also differing only in the counterion, show a similar result (0.020 Å). These anion-related differences are much smaller (≤25%) than the differences arising from the identity of the metal atom (Ag vs Au). On the basis of these data, it seems reasonable to assume that the identity of a noncoordinated anion does not significantly affect the M–P bond lengths and therefore that the identity of the anion may be disregarded. Likewise, as long as there are no significant sub-van der Waals contacts, the solid-state packing does not seem to affect the M–P bonding significantly. Therefore, the pairs of compounds do not need to be isomorphous in order to make a useful comparison. Using these criteria, the database search yielded 13 pairs of isostructural complexes (Table 7). These results include two pairs of complexes that are not perfectly isostructural. (1) The two complexes incorporating the thiocyanate ligand are “linkage isomers”, and 2) the Ph<sub>3</sub>PAuNO<sub>3</sub> is strictly two-coordinate, while the corresponding silver complex forms additional long Ag–O interactions. However, these two pairs of complexes were included because the bond lengths as well as the bond length differences observed for them are consistent with those seen in the other pairs. Overall, the observed Au–P bond length is indeed shorter than the corresponding Ag–P bond length with the differences ranging from 0.065 to 0.169 Å and an average difference of 0.120 Å. Considering the diversity of structures represented in this collection, the average value agrees very well with the theoretical prediction (0.093 Å), which is based on a linear two-coordinate model. Indeed, if only the truly two-coordinate complexes (i.e., excluding the Ph<sub>3</sub>PMNO<sub>3</sub> complexes) are considered, the average value for the difference is 0.093 Å, in perfect agreement with theory.

## Conclusions

This work shows that it is possible to prepare and isolate low-coordinate phosphine complexes of silver(I) without the use of sterically bulky ligands. Furthermore, such coordinatively unsaturated complexes can persist in solution indefinitely in the absence of any additional Lewis bases. In light of this finding, we are presently investigating the use of **I** and **II** as synthons

- (27) Staples, R. J.; King, C.; Khan, Md. N. I.; Winpenny, R. E. P.; Fackler, J. P., Jr. *Acta Crystallogr.* **1993**, *C49*, 472–475.
- (28) Jones, P. G. *J. Chem. Soc., Chem. Commun.* **1980**, 1031–1033.
- (29) Jones, P. G.; Sheldrick, G. M.; Muir, J. A.; Muir, M. M.; Pulgar, L. B. *J. Chem. Soc., Dalton Trans.* **1982**, 2123–2125.
- (30) (a) Muir, J. A.; Muir, M. M.; Arias, S.; Campana, C. F.; Dwight, S. K. *Acta Crystallogr.* **1982**, *B38*, 2047–2049. (b) Muir, J. A.; Muir, M. M.; Arias, S.; Jones, P. G.; Sheldrick, G. M. *Inorg. Chim. Acta* **1984**, *81*, 169–174.
- (31) Harker, C. S. W.; Tiekink, E. R. T. *J. Coord. Chem.* **1990**, *21*, 287–293.
- (32) Bates, P. A.; Waters, J. M. *Inorg. Chim. Acta* **1984**, *81*, 151–156.
- (33) Jones, P. G. *Acta Crystallogr.* **1980**, *B36*, 3105–3107.
- (34) Bowmaker, G. A.; Dyason, J. C.; Healy, P. C.; Engelhardt, L. M.; Pakawatchai, C.; White, A. H. *J. Chem. Soc., Dalton Trans.* **1987**, 1089–1097.
- (35) Khan, Md. N. I.; Staples, R. J.; King, C.; Fackler, J. P., Jr.; Winpenny, R. E. P. *Inorg. Chem.* **1993**, *32*, 5800–5807.
- (36) Jones, P. G. *Z. Kristallogr.* **1995**, *210*, 896.
- (37) Guy, J. J.; Jones, P. G.; Sheldrick, G. M. *Acta Crystallogr.* **1976**, *B32*, 1937–1938.
- (38) Camalli, M.; Caruso, F. *Inorg. Chim. Acta* **1988**, *144*, 205–211.
- (39) (a) Cooper, M. K.; Dennis, G. R.; Henrick, K.; McPartlin, M. *Inorg. Chim. Acta* **1980**, *45*, L151–L152. (b) Muir, J. A.; Muir, M. M.; Pulgar, L. B.; Jones, P. G.; Sheldrick, G. M. *Acta Crystallogr.* **1985**, *C41*, 1174–1176.
- (40) Liu, C. W.; Pan, H.; Fackler, J. P., Jr.; Wu, G.; Wasylshen, R. E.; Shang, M. J. *J. Chem. Soc., Dalton Trans.* **1995**, 3691–3697.
- (41) Khan, Md. N. I.; King, C.; Fackler, J. P., Jr.; Winpenny, R. E. P. *Inorg. Chem.* **1993**, *32*, 2502–2505.
- (42) Karsch, H. H.; Schubert, U. Z. *Naturforsch.* **1982**, *B37*, 186–189.
- (43) (a) Payne, N. C.; Puddephatt, R. J.; Ravindramath, R.; Treurnicht, I. *Can. J. Chem.* **1988**, *66*, 3176–3183. (b) Perreault, D.; Drovín, M.; Michel, A.; Miskowski, V. M.; Schaefer, W. P.; Harvey, P. D. *Inorg. Chem.* **1992**, *31*, 695–702.
- (44) (a) Barron, P. F.; Engelhardt, L. M.; Healy, P. C.; Oddy, J.; White, A. H. *Aust. J. Chem.* **1987**, *40*, 1545–1555. (b) Wang, J.-C.; Khan, Md. N. I.; Fackler, J. P., Jr. *Acta Crystallogr.* **1989**, *C45*, 1008–1010.

for the rational synthesis of new mixed-ligand complexes of silver. Last, both the structural work and the database analysis presented here strongly support the theory proposed elsewhere that the covalent radius of gold is approximately 0.1 Å smaller than that of silver.

**Acknowledgment.** This work was supported by Georgetown University and the donors of the Petroleum Research Fund, administered by the ACS. The purchase of the X-ray diffrac-

tometer was made possible by a grant from the National Science Foundation (CHE-9115394).

**Supporting Information Available:** Complete crystallographic information for **I**·0.5CH<sub>2</sub>Cl<sub>2</sub> and **II** including tables of positional and equivalent displacement parameters, bond metrics, and anisotropic displacement parameters, in CIF format, is available through the Internet only. Access information is given on any current masthead page.

IC980726K